Check for updates

Received: 6 June 2023 | Revised: 31 August 2023 | Accepted: 14 October 2023

DOI: 10.1002/nme.7410

RESEARCH ARTICLE

WILEY

Towards the saving potentials using a hybrid topology optimization: Application of a coupled deterministic and empirical approach solving a geotechnical optimization problem

Elnaz Hadjiloo | **Stefanie Knutz** | **Jürgen Grabe**

Institute of Geotechnical Engineering and Construction Management, Hamburg University of Technology (TUHH), Hamburg, Germany

Correspondence
Elnaz Hadjiloo, Institute of Geotechnical Engineering and Construction Management, Hamburg University of Technology (TUHH), Harburger Schloßstraße 36, 21079, Hamburg, Germany.
Email: elnaz.hadjiloo@tuhh.de

Abstract

This article presents the application of the TOSS (topology optimization for stiffness and strength) algorithm, a hybrid optimization strategy for topology optimization, used for the design of a strip foundation as a basic geotechnical structure. One of the challenges of this field is to improve structural performance by using less material than conventional structures. Therefore, the SIMP (solid isotropic material with penalization) is applied to optimize the foundation concerning its deformational behavior. The downstream SKO (soft kill option) then solves for optimality concerning the foundation's stress distribution. Numerical experiments with the TOSS algorithm reveal great potential for material savings. The coupled solution presents the benefit of reducing CO_2 emissions due to material savings of more than 20% in comparison to the individual SIMP and SKO algorithms. A positive by-product of the method is that stress peaks under the foundation are reduced due to the homogenization of stresses as a result of SKO optimization, thus creating the conditions for better durability of the foundation.

KEYWORDS

hybrid topology optimization, SIMP, SKO, topology optimization, TOSS

1 | INTRODUCTION

In general, optimization can be defined as the process of determining a more optimal solution to a defined problem.[1] With respect to this article, optimization is used to find a more optimal solution for a strip foundation considering a specific load case.

Optimization can be used wherever there is potential for improvement. Determining the most suitable optimization approaches highly depends on the regime of the optimization problem, the entity subject for optimization, and the constraints.[2] If structural optimization is considered independent of the optimization approaches used, it can generally be divided into three areas: dimensioning, shape, and topology optimization (e.g., in Figure 1). The three areas of structural optimization contribute to the optimized design parameters. Constraints, for example, in terms of the control for the

This is an open access article under the terms of the Creative Commons Attribution-NonCommercial License, which permits use, distribution and reproduction in any medium, provided the original work is properly cited and is not used for commercial purposes.
© 2023 The Authors. *International Journal for Numerical Methods in Engineering* published by John Wiley & Sons Ltd.

geometry, can be implied by the extension of the optimization problem. They can be distinguished by the parameterization of the optimization problem, which is determined by the definition of the design parameters.[3]

Current high-performance computing utilizes mature techniques developed in the 1980s and the continuous development of optimization techniques remains crucial for engineering objectives.[4] Common objectives in geotechnical engineering mainly relate to structural enhancements or deal with economic performance. Additionally, sustainable construction is becoming increasingly important. Saving material, thus saving weight, costs, and emissions, can contribute to this goal. By applying new calculation methods, optimization can be applied to a wider range of objectives and diverse goals. With respect to the geotechnical context of strip footing in this article, objectives identified for optimization vary from simplistic formulation (mass and compliance) to extensive formulations respecting probabilistic effects (e.g., uncertainties in stress states or E-modules).

In contrast to dimensioning and shape optimization, topology optimization does not require a specific start design of the topology. With that, it provides answers to one of the most fundamental questions in engineering: How should material be placed within a specific design area to achieve the best structural performance in terms of an underlying objective?[5] Topology optimization only requires a design space Ω in which the structure is to be placed. Therefore, $\Omega_0 = \boldsymbol{x} \in \mathbb{R}$ (cf. Figure 1) is set at the beginning of the optimization.[6] As a branch of mathematics, the topology describes the location and arrangement of individual elements of a structure, which can significantly influence the behavior of the structure. In topology optimization, the topological properties and thus the most general geometric properties of a structure are changed, which is why this process should take place at an early design stage. Most methods of topology optimization try to determine a design proposal by respecting, for example, a combination of Dirichlet and Neumann boundary conditions.[3] With that, topology optimization is a very general form of structural optimization and often includes shape optimization (cf. Γ Figure 1) and dimensioning (cf. l Figure 1) due to its design parameter Ω.

According to Harzheim,[2] if topology optimization methods are generally considered according to their approach to solving the problem, two distinct groups are stated by Harzheim,[2] deterministic and stochastic solution strategies. The former are based on deterministic functional analysis fundamentals for solving the minimization problem, whereas the latter are based on probabilistic formulations.[2] There are various methods within topology optimization, such as the BESO (bidirectional evolutionary structural optimization) and SKO (soft kill option) methods, both using stochastic solution strategies, or SIMP (solid isotropic material with penalization) an often used deterministic method. Furthermore, there are methods that can be broadly categorized as topology optimization. Examples of these are the Level-Set and Phase-Field methods. These latter methods utilize the variation of structural boundaries in the optimization process. In contrast to density-based approaches that explicitly parameterize the entire design space, implicit functions are employed to describe and adjust the structural boundaries. The Phase-Field method utilizes the development of a two-phase field to classify solid and void regions. The Level-Set method uses the so-called Level-Set function to describe the material boundary.[7] However, when the Level-Set method is combined with other methods, for instance, the bubble method by Eschenauer,[8] void regions can be introduced into the structure prior to the application. During optimization, not only does the outermost structural boundary change but also the boundaries of the inner void regions can vary. This could involve altering the shape of void regions or merging individual void regions. This approach, unlike traditional shape optimization where only the outer structural boundary changes, allows for the creation and shaping of voids or holes within the structure. As a result, it finds application in topology optimization.[7] On the other hand, the BESO method is a topology optimization technique used to find the optimal distribution of material within a given design domain in

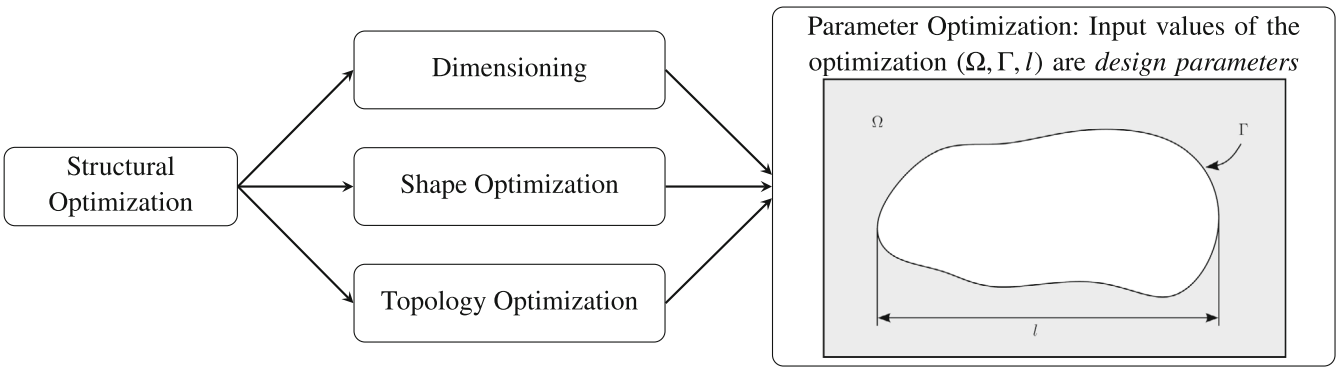

FIGURE 1 Classification of structural optimization based on parameterization.

10970207, 2024, 6, Downloaded from https://onlinelibrary.wiley.com/doi/10.1002/nme.7410 by Technische Universität Hamburg Universitätsbibliothek, Wiley Online Library on [04/03/2025]. See the Terms and Conditions (https://onlinelibrary.wiley.com/terms-and-conditions) on Wiley Online Library for rules of use; OA articles are governed by the applicable Creative Commons License

order to achieve specific performance objectives. It's particularly useful for structural design problems where the goal is to determine the optimal layout of material to minimize structural compliance or maximize stiffness while satisfying certain constraints. This method is effective for problems with discrete loading conditions, such as truss and frame structures. However, it may not be as suitable for problems with continuous loading or complex material behavior. The key feature of BESO is its iterative approach that involves adding and removing material from the design domain based on the material densities.[9] A common deterministic approach for topology optimization is the SIMP approach, which aims to minimize the compliance of a structure, by optimizing its stiffness to the given load case. This method was proposed by Bendsøe[10] and popularized by the article, "A 99 line topology optimization code written in Matlab" by Sigmund[11] the SIMP approach became generally accepted in the field of topology optimization. The potential of it could be shown in a wide range of applications in various fields (cf. References 12–14), as well as in the field of geotechnics, compare References 6 and 15. SKO is an empirical method of topology optimization that aims to optimize the distribution of stresses within a structure. With its origins in bionics, the SKO approach follows the objective of ensuring a high level of failure safety with minimal material use. This is achieved by using a homogeneous stress distribution within the structure. For this reason, the SKO method is of great interest due to the potential for material saving, and the wide range of applicable disciplines (cf. References 16–18). Due to increasing material costs and the demand for reducing emissions, material savings are highly important in the construction industry, therefore making the SKO approach appealing. The TOSS (topology optimization for stiffness and stress) method, as it was named by Frisch[19] combines both objects of the previously mentioned optimization approaches. This method minimizes compliance and maximizes the strength of a structure sequentially. TOSS is a hybrid method of topology optimization by combining two different optimization objectives.[19] The purpose of this contribution is to investigate if the hybrid optimization algorithm TOSS leads to greater saving potential regarding the volume and thus material of a structure compared to conventional mono criteria algorithms like SIMP and SKO. In the following, a strip foundation is investigated as a boundary value problem using both, the SIMP and TOSS method. The volume and density of each method were determined and compared to evaluate the material consumption. This article begins with a brief introduction to the theoretical background of the optimization methods in Section 2. First, the general SIMP method is presented in Section 2.1 followed by the general method of the SKO in Section 2.2. Section 2.3 explains the theoretical background of the TOSS algorithm, including the necessary modifications made in the course of this work. Both the general forms of the SIMP and SKO methods were adapted and a coupling of these was implemented. In Section 3, the numerical setup of the investigated strip foundation is described. Following this, Section 4 will present the results of the numerical simulations of the coupled optimization and compare them briefly to the standalone SIMP and SKO optimizations. This article concludes with Section 5, a brief discussion of the major findings. The numerical simulations are carried out with the commercial software MATLAB coupled with ABAQUS.

2 | THEORETICAL BACKGROUND

In the following subsections, a brief introduction to SKO and SIMP, and the theoretical background of the optimization methods are described. For more detailed information on the optimization approaches themselves, the authors refer to, for example, Baumgartner et al.[18] for the SKO approach and Sigmund[11] for SIMP. The last Section 2.3 gives a theoretical background on how the combined hybrid optimization is implemented. Implied adjustments and modifications to suit the application in a geotechnical environment are presented in the second part of this Section 3.

2.1 | SIMP method

Background knowledge on the principles used by the SIMP approach was provided by Bendsøe.[20] Later, the approach became popularized by the open source publication "A 99 line topology optimization code written in Matlab" by Sigmund.[11] It serves today as a great model on this topic. Work such as that of Reference 15, 21, or 6 already show that the SIMP approach is suitable for optimizing the bearing capacity of geotechnical constructions. The topology of the geotechnical construction is hereby described by values of a parameter called virtual material density $\boldsymbol{x}$, which are referred as control of the following problem. The design space is discretized with finite elements. Material parameters are assigned to each element, depending on the virtual material density. At the beginning of the optimization, the available material for construction optimization is evenly distributed in the design space. Virtual material distribution is assigned to the loaded areas, whereas in unloaded areas of the design space, less virtual material is assigned.[22]

10970207, 2024, 6, Downloaded from https://onlinelibrary.wiley.com/doi/10.1002/nme.7410 by Technische Universität Hamburg Universitätsbibliothek, Wiley Online Library on [04/03/2025]. See the Terms and Conditions (https://onlinelibrary.wiley.com/terms-and-conditions) on Wiley Online Library for rules of use; OA articles are governed by the applicable Creative Commons License

As a result of the compaction and loosening the virtual density of the elements, a foundation structure is formed. The virtual material distribution with $\boldsymbol{x}_e \in [0,1]$ defines how dense an element is. The mapping per element is given in Equation (1).

$$x_e = \begin{cases} 0 & \rightarrow & \text{soil} \\ 0 < x_e < 1 & \rightarrow & \text{mixed material of soil and concrete} \\ 1 & \rightarrow & \text{concrete.} \end{cases} \tag{1}$$

SIMP is applied to minimize the compliance c of the underlying structure. As a function of the design variable $\boldsymbol{x}$, the objective of the optimization is defined as:

$$c(\boldsymbol{x}) = \boldsymbol{u}^{\mathrm{T}}\boldsymbol{K}\boldsymbol{u}. \tag{2}$$

As described in Equation (2) minimizing the compliance requires increasing the system stiffness $\boldsymbol{K}$ or a reduction of the displacement $\boldsymbol{u}$. Both of these imply an increase in the corresponding bearing capacity of a geotechnical structure. Since the applicable problem is a discretized physical system, the compliance of the whole system is the sum of the compliance of all n elements in the design space. In order to avoid a convergence towards a trivial solution which is a design space filled with concrete, additional constraints are implied. The first constraint requires equilibrium conditions at all times. The second constraint describes the radio d of the structural volume $v(\boldsymbol{x})$ (concrete) to the volume of the total design space $v^0(\boldsymbol{x}) = 0$. The third is a constraint on the control and ensures the mapping given in Equation (1). The resulting optimization problem reads

$$\begin{cases} \min: & c(x) = \boldsymbol{u}^{\mathrm{T}}\boldsymbol{K}\boldsymbol{u} = \sum_{e=1}^{n}(x_e)^p u_e^{\mathrm{T}}\boldsymbol{K}_0 u_e \\ \text{s.t.} \begin{cases} & \boldsymbol{K}\boldsymbol{u} = \boldsymbol{f} \\ & \dfrac{v(\boldsymbol{x})}{v^0(\boldsymbol{x})} = d \\ & 0 \le x_e \le 1. \end{cases} \end{cases} \tag{3}$$

Beside the global displacement vector $\boldsymbol{u}$ and the global stiffness matrix $\boldsymbol{K}$, $\boldsymbol{u}_e$ is the element displacement and $\boldsymbol{K}_0$ is the element stiffness matrix of the initial structural material. The density distribution of the individual elements is given by x_e. If x_e is 1, the element is completely filled with the structural material (high density). During the optimization process, the material distribution in the design space changes, with the aim to create a topology whose compliance is as low as possible. In this process, the virtual density of the elements changes to ensure the elements take values between 0 and 1, meaning that there is a mixed material of soil and concrete. Since a constructional realization of these intermediate materials is not possible, a discretization of the virtual material density is achieved by exponentiating the virtual material density with the penalty term p.[6] According to Bendsøe[10] p should be ≥ 3 in a two-dimensional space. By this penalty term the material transition is accelerated and thus the occurrence of intermediate materials is prevented. Figure 2 illustrates the relationship between the virtual element density x_e and the ratio of the stiffness of the soil material E_0 and the element stiffness E_1 as a function of the penalty term p. Thus, the element stiffness matrix $\boldsymbol{K}_e$ can be defined by the following equation

$$\boldsymbol{K}_e = (x_e)^p \boldsymbol{K}_0. \tag{4}$$

Since there is a risk with a too strong penalty factor in the first iteration steps, because it leads to a stiffening of the algorithm and thus no global optimum is found, the penalty factor is increased with increasing iteration steps (cf. Table 1). This procedure is called continuation method according to Rozvany.[23]

The derivative $\partial c/\partial x_e$ of the objective $c(\boldsymbol{x})$ describes the influence of a small change in x_e on the cost function and is referred as sensitivity. It is given by

$$\frac{\partial c}{\partial x_e} = \sum_{e=1}^{n} - p(x_e)^{p-1} \boldsymbol{u}_e^T \boldsymbol{K}_0 \boldsymbol{u}_e. \tag{5}$$

10970207, 2024, 6, Downloaded from https://onlinelibrary.wiley.com/doi/10.1002/nme.7410 by Technische Universität Hamburg Universitätsbibliothek, Wiley Online Library on [04/03/2025]. See the Terms and Conditions (https://onlinelibrary.wiley.com/terms-and-conditions) on Wiley Online Library for rules of use; OA articles are governed by the applicable Creative Commons License

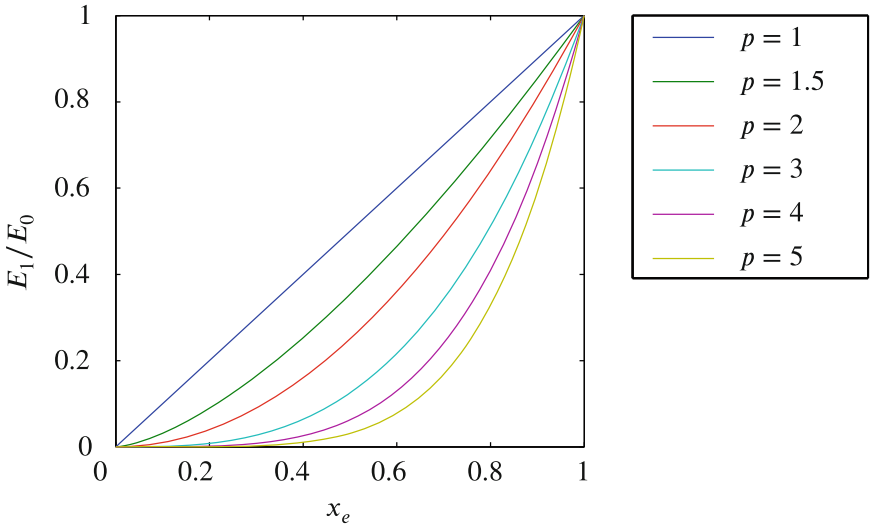

FIGURE 2 Description of the material transition E_1/E_0 at different element densities x_e under the application of different penalty terms p using SIMP according to Reference 7.

TABLE 1 Application of the *continuation method* to the penalty term p.

Iteration k	<10	11–20	21–30	31–40	>40
Penalty term p	1	2	3	4	5

The optimality conditions by Bendsøe[10] deliver an approximation to the solution of Equation (3). Hereby, the material distribution is updated at each iteration step using a heuristic approach, with a limit, which is defined in Equation (6).

$$x_e^{\text{neu}} = \begin{cases} \max(x_{\min}, x_e - m), & \text{if } x_e B_e^{\eta} \leq \max(x_{\min}, x_e - m), \\ x_e B_e^{\eta}, & \text{if } \max(x_{\min}, x_e - m) < x_e B_e^{\eta} < \min(1, x_e + m), \\ \min(1, x_e + m), & \text{if } \min(1, x_e + m) \leq x_e B_e^{\eta}. \end{cases} \tag{6}$$

The numerical damping coefficient $\eta = 0.5$ and the movement limit $m = 0.2$ are chosen to create a numerically stable system to generate an efficient solution. The coefficient m limits possible changes in the virtual material distribution in every iteration step. B_e is determined using the Lagrange-multiplier λ, the sensitivity $\partial c/\partial x_e$ and the volume limitation of V as

$$B_e = \frac{-\frac{\partial c}{\partial x_e}}{\lambda \frac{\partial V}{\partial x_e}}. \tag{7}$$

The Lagrange-multiplier λ is calculated with the bisection method.[2] By using this method, the requirements regarding the volume in the optimization problem are fulfilled. The requirement on the virtual material density is implemented in the optimality criteria. By using the implicit finite element method (FEM), the physical constraint $\boldsymbol{Ku} = \boldsymbol{f}$ is fulfilled. Due to the discretization used in the application of the SIMP approach, the problem of *checkerboarding* may occur. If some elements filled with structural material are connected only by their corner nodes, they form a checkerboard pattern, leading to an overestimation of stiffness.[23] To perform the optimization independently of the discretization, different techniques, as listed in Reference 7 or 11, can be used to reduce the *checkerboarding*.

2.2 | SKO method

The topology optimization approach SKO originated from the field of bionics and embodies the biological growth rule. This rule aims to create the highest possible failure safety using the least amount of material as possible. The investigation

10970207, 2024, 6, Downloaded from https://onlinelibrary.wiley.com/doi/10.1002/nme.7410 by Technische Universität Hamburg Universitätsbibliothek, Wiley Online Library on [04/03/2025]. See the Terms and Conditions (https://onlinelibrary.wiley.com/terms-and-conditions) on Wiley Online Library for rules of use; OA articles are governed by the applicable Creative Commons License

of various biological force carriers resulted in the hypothesis that the structures grow into such a form in which a homogeneous stress distribution is formed on the surface of the structure.[2] By applying the effect of adaptive bone mineralization, also the SKO approach, which was developed by Baumgartner,[18] targets this condition. Thereby, areas or elements in which higher stresses occur are strengthened and vice versa. Conversely, elements with lower stresses are weakened. Thus, the stiffness of the material is adjusted depending on the stress distribution. This process, by default, is implemented by modifying the Young's modulus of the individual elements directly.[18]

Normally, in finite element analysis (FEA) interaction is calculated via a scalar field, for example, T. The Young's modulus of all elements is then interpolated between $T_{\min}$ and $T_{\max}$ using the scalar field, as Figure 3 (gray line) shows. The bounds $T_{\min}$ and $T_{\max}$ depend on the sizes chosen for the scalar field. The introduced quantities have no physical meaning and merely serve to control the Young's modulus of the individual elements, since these can be defined as a function of the scalar field in the FEA. Elements with low values of T are associated with low Young's modulus, ultimately resulting in a void. Between these values, a linear relationship can be assumed (cf. Figure 3).[2]

The material properties are adjusted depending on this relation. By modifying the properties of the elements, lower strain changes are expected at constant stresses. In conventional SKO, linear-elastic material behavior is considered with $E_{\text{mod}} = \Delta\sigma/\Delta\epsilon$. It is important to note that stresses change during topology optimization, as the area of the structure A is not constant. This occurs even when the applied force F remains constant, resulting in $\sigma = F/A$. Nevertheless, the homogenization of the stress distribution of the structure contributes to increased stiffness of the structure in areas of high loads. Baumgartner[18] defines different ways to include the stress distribution by modifying the Young's modulus. The process of mineralization, in the frame of this work, shows the best convergence. This process defines, according to Harzheim,[2] the value $T_i^{(k+1)}$ in the iteration step $k+1$ for every node i with

$$T_i^{(k+1)} = T_i^{(k)} + s\left(\sigma_i^{(k)} - \sigma_{\text{ref}}\right). \tag{8}$$

Here s is the scale factor, σ_i is the stress in the node i and σ_{ref} is the defined reference stress, which specifies if a node is loaded ($\sigma_{\text{ref}} < \sigma_i$) or not loaded ($\sigma_{\text{ref}} > \sigma_i$). $T_i^{(k)}$ defines the values of the scalar field of the previous iteration step of all nodes i and underlies the following constraints:

$$T_i^{(k)} = \begin{cases} T_{\max} & \text{if} \quad T_i^{(k)} > T_{\max} \\ T_{\min} & \text{if} \quad T_i^{(k)} < T_{\max} \\ T_i^{k} & \text{else.} \end{cases} \tag{9}$$

It should also be noted that a smaller stress is assumed for the reference stress σ_{ref} at the beginning of the optimization. The reason for this assumption is due to the high stress in large areas is lower than the target value of the reference stress, and thus a large part of the material is removed immediately. If the model begins at lower stress and slowly to the reference stress, a structure can be expected to form along the force flow as desired.[2]

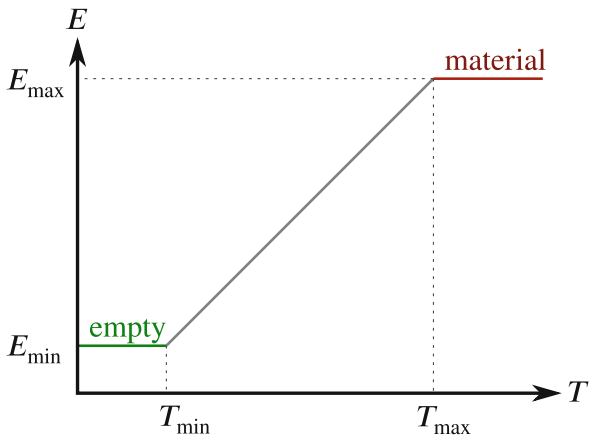

FIGURE 3 Relationship between the temperature (T) and the Young's modulus (E) related to each element.[2]

10970207, 2024, 6, Downloaded from https://onlinelibrary.wiley.com/doi/10.1002/nme.7410 by Technische Universität Hamburg Universitätsbibliothek, Wiley Online Library on [04/03/2025]. See the Terms and Conditions (https://onlinelibrary.wiley.com/terms-and-conditions) on Wiley Online Library for rules of use; OA articles are governed by the applicable Creative Commons License

2.3 | Developed hybrid algorithm

In addition to the individual optimization approaches like SIMP or SKO it is also possible to use a combined optimization approach. The topology optimization for stiffness and strength (TOSS) method, as presented by Frisch[19] and Rosnitschek[24] is a hybrid optimization method of the SIMP approach and the SKO approach. The first successful application of this combined optimization was in the field of adaptive manufacturing. In this article, it will be shown, that the application of this combined optimization creates benefits for the geotechnical problem. The optimality criterion used in the SIMP method is used to optimize the structure with respect to its stiffness (compliance with respect to this article). As soon as an optimal solution is obtained, the SKO algorithm is subsequently applied to optimize the strength (homogeneous stress state). Thus, the objective of the TOSS method is to minimize the compliance and to create a homogeneous stress state. Since there are two objectives for optimization, the TOSS method is considered a multi-criteria optimization method that runs sequentially and not simultaneously. The state of the system is evaluated with each iteration step using the FEA. The first optimization method is stopped as soon as the defined termination criterion is reached. After that, the second optimization method is applied, which again will stop as soon as a defined termination criterion is reached. In order to carry out the SKO algorithm as an extension of the SIMP algorithm and apply the hybrid algorithm to a geotechnical boundary problem, specific adjustments are necessary. Unlike with the conventional SKO method, in this method, no control of the Young's modulus is used. The reason for this is due to the adoption of the hypoplastic soil model by Pucker[15] which considers the material transition from soil to concrete. Instead of the distribution of the Young's modulus, the distribution of the virtual density is considered in the optimization process and connected to the soil model by transferring the calculated virtual density as an interpolation factor to the soil model.

In the framework of this method, the virtual density is a scalar field representing the material distribution of soil and structural material (concrete) and is used in both the SIMP algorithm and the SKO algorithm. The virtual density x is used as a node-wise value in ABAQUS for both cases. In MATLAB the element-wise formulation of x_e is used to determine the better solution with the SIMP optimization. The SKO optimization uses a node-wise formulation of the virtual density x_i during the calculations. Transformations from element (e) to node values (i) are calculated by interpolation. Replacing the use of the Young's modulus by using a virtual density is efficient because fewer interpolation steps are required. This process of replacement starts with using the Young's modulus. When using Young's modulus, the element output stresses from ABAQUS have to be extrapolated to the nodes of the respective element. Based on the stresses at the nodes, interpolation factors can be calculated. The calculated factors must be interpolated into elements because the resulting distribution of the Young's modulus is defined element-wise. The element-wise values must be transformed into nodes because the virtual density is defined node-wise. By directly considering the virtual densities and transferring them as an interpolation factor to the soil model optimizes interpolation steps, compare Figure 4, compared to using the interpolation of the Young's modulus. It is necessary to reduce the element-wise stress distribution from the FEA to nodes (node-wise) in order to carry out the calculations of the new virtual density (node by node) in MATLAB. In the following Figure 4 the interpolation procedure using the adopted SKO optimization is shown in black. The steps are depicted in gray, however they are no longer required due to the modifications.

Using the virtual density as a scalar field for the SKO algorithm leads to the fact that the equation for the update of the densities compare Equation (8) can be written in the following form,

$$x_i^{(k+1)} = x_i^{(k)} + s\left(\sigma_i^{(k)} - \sigma_{\text{ref}}\right). \tag{10}$$

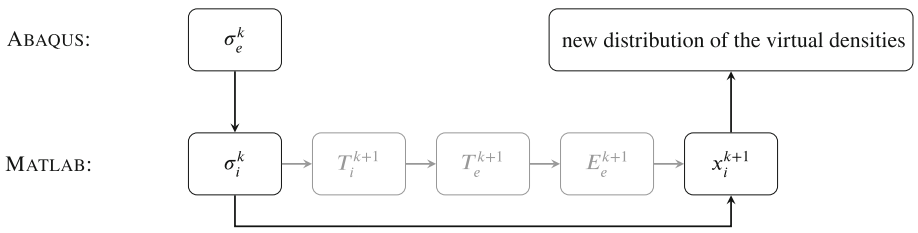

FIGURE 4 Interpolation procedure applying the adapted SKO optimization (black) for the hybrid optimization in comparison to the required steps, using the conventional SKO optimization (gray).

10970207, 2024, 6, Downloaded from https://onlinelibrary.wiley.com/doi/10.1002/nme.7410 by Technische Universität Hamburg Universitätsbibliothek, Wiley Online Library on [04/03/2025]. See the Terms and Conditions (https://onlinelibrary.wiley.com/terms-and-conditions) on Wiley Online Library for rules of use; OA articles are governed by the applicable Creative Commons License

The scaling factor s, as well as the existing stress of each element σ_e (interpolated to nodes σ_i) and the fixed reference stress σ_{ref} maintain their original meaning, whereby the node stresses are approximated from elements to nodes analogous to the introduced interpolation and extrapolation approaches. To ensure that the influence of the stress difference ($\sigma_i^{(k)} - \sigma_{ref}$) behaves appropriately to the virtual density, the scaling factor s should be adjusted. The work of Frisch[19] shows that the scaling factor for the mentioned temperature field with $s = 2$ gives appropriate results and scales the influence well. Since the values for the virtual density are approximately one hundredth as large as those of the temperature field mentioned, it is suggested to scale the scaling factor likewise to s = 2/100. Initially, the scaling factor is assumed to be the same however, the scaling factor must be adapted to the specific boundary value problem in each case. Once applied to the virtual density, new conditions are defined for the constraints listed in (9). these result in

$$x_i^{(k)+1} = \begin{cases} 1 & \text{if} \quad x_i^{(k)} > 1 \\ 0 & \text{if} \quad x_i^{(k)} \leq 0 \\ x_i^k & \text{else.} \end{cases} \tag{11}$$

For the implementation of a hybrid algorithm considering both the SIMP and the SKO algorithms, both methods must be connected. First, the SIMP approach minimizes the compliance c of the structure, and then the SKO approach aims for a homogeneous stress distribution. The result of the SIMP approach is used as the starting solution for the SKO approach is not an initial value of $x_i^0 = 1$ as usual. According to this, the starting design of the SKO optimization ($x_{SKO,i}^1$) uses the material distribution the material distribution from the last SIMP optimization ($x_{SIMP,i}^{last}$).

Based on the last iteration of the SIMP optimization, a distribution of the virtual density in the design space, is further optimized by the SKO optimization. Using this method implemented with $x_i = 1$ is an advantage because it eliminates difficulties with the initial estimations. Typical models require an initial estimation that may lead to steering the model in one subjective direction. Based on this stress distribution, the reference stress σ_{ref} is determined and the initial state of the material distribution is generated. Starting with the first iteration step of the SKO optimization, the structure optimized for minimizing compliance is then further optimized according to the SKO approach. Initial calculations with the TOSS algorithm have shown that part of the optimization with the SKO algorithm tends to converge with increasing iteration steps. The SKO algorithm converges to trivial solutions, as the stress state becomes its maximized homogenous state. In this case, the design space is either completely filled with structural material (reference stresses selected too low), or no structural material is placed in the design space at all (reference stresses selected too high). It could be observed that the compliance, which is optimized by the SIMP approach, is either extremely increasing ($x_i = 0$) or decreasing ($x_i = 1$). This behavior of the SKO approach may occur due to a missing constraint for the volume since the compliance c of the system correlates with the development of the volume. Finally, the increase in volume results in the increase of the structural material, which has a higher stiffness than the soil and thus decreases the compliance. For this reason, a new constraint is implemented to ensure changes in the optimized compliance remain small and limit the change in volume. By executing this new constraint, the optimality with regard to the compliance c is not completely discarded. As a result of this, the update of the virtual density x_i is extended by an additional term and results in

$$x_i^{(k+1)} = \underbrace{x_i^{(k)}}_{\text{current virt. density}} + \underbrace{s\left(\sigma_i^k - \sigma_{ref}\right)}_{\text{SKO-update}} - \underbrace{\rho_c\left(c_{SIMP} - c_{curr}^{(k)}\right)}_{\text{constraint}}. \tag{12}$$

The last term in Equation (12), "constraint," has an influence on the update of the virtual density x_e, if the current averaged compliance ($c_{curr}^{(k)}$) changes strongly compared to the averaged compliance of the last SIMP calculation (c_{SIMP}). The factor ρ_c, has magnitude as listed in Table 2 depending on the iteration k and controls the influence of that constraint on the virtual density. Through the introduction of the additional constraint, the optimization problem changes compared to the conventional application of the SKO optimization. The decisive update is still to be influenced by the "SKO Update." Heuristic investigations have shown that the factors listed in Table 2 are suitable for scaling the influence of the constraint.

TABLE 2 Used factors ρ_c for scaling the constraints of the SKO-optimization.

Iteration k	<30	<50	<100
Scaling ρ_c	10	20	25

10970207, 2024, 6, Downloaded from https://onlinelibrary.wiley.com/doi/10.1002/nme.7410 by Technische Universität Hamburg Universitätsbibliothek, Wiley Online Library on [04/03/2025]. See the Terms and Conditions (https://onlinelibrary.wiley.com/terms-and-conditions) on Wiley Online Library for rules of use; OA articles are governed by the applicable Creative Commons License

When comparing to the virtual density x, whose definition range is between 0 and 1 and operates by updates from the SKO optimization, the influence of the constraint differs from that of the virtual density by about one-tenth. The constraint does not have a great influence on the current update. By increasing ρ_c from the 30th or 50th iteration onwards, convergence behavior develops with each increasing iteration. As a result, the stress differences decrease with increasing iteration. The introduction of this constraint prevents the occurrence of trivial solutions. This additional constraint simplifies the choice of the reference stress σ_{ref} since the system itself can react if the chosen reference stress is too high or too low.

3 | NUMERICAL SETUP

In the following, the numerical setup of the boundary value problem is presented. The geotechnical problem considered is a strip foundation that must be optimized in terms of its deformation behavior and stress distribution. The implementation of the strip foundation in ABAQUS is presented, as well as the setup of the optimization algorithm. A hypoplastic material model is employed. In the case of hypoplastic material models, there is generally a nonlinear incremental relationship considered between stresses and strains. Such material models are widely used in geotechnical engineering for a more precise description of materials like sands. A significant advantage of hypoplastic material models is that the evolution of pore volume is taken into account, which plays a crucial role in soils. In the context of this study, a hypoplastic material model based on the general formulation by Niemunis,[25] with extensions by Pucker,[15] was utilized. These extensions enable the representation of a continuous material transition from an unstrengthened soil to a strengthened soil. The strengthening takes place while considering material properties of concrete and, in this case, represents the structural material. Hence, the material model is capable of representing both the soil and the structural material within a single model. The material parameters of both materials were introduced by Pucker.[15] For the soil, the parameters of the "Wundersand" are used and the foundation material consists of a concrete-sand mixture. The material parameter used for the hypoplastic soil model are shown in Table 3.

3.1 | Boundary value problem: Strip foundation

The hybrid optimization algorithm is applied to a strip foundation as a boundary value problem. The FE model of the strip foundation is shown in Figure 5. The modeling and discretization are done in ABAQUS (using a solution domain $A \subset \mathbb{R}^2$), using plain strain conditions. To reduce the computational effort the symmetry of the model is used, therefore only one-half of the model is discretized and used for the calculation. The modeled solution space has a width of 6m and a depth of 7m. The uniformly finely discretized design space ($D \subset A$) is 2m wide and has a depth of 3m. This area is available during optimization for the formation of a topology. An adjustment of the virtual density is made to make the associated parameters possible in this area. Each element in the design space has an edge length of 5cm. Elements of the type CPE4 are used. These are elements with linear approach functions and four support points each for Gaussian integration.[26] The area outside the design space is not addressed by the optimization and is only used to implement the Dirichlet and Neumann boundary conditions. Additionally, this area remains unchanged as soil material, that is, always has a virtual density of $\boldsymbol{x} = 0$ according to Equation (1). This area is also discretized with the elements mentioned, but the edge length varies. The element size increases with the distance to the design space Ω, since a fine discretization is not of high priority in this application, and computing capacity can be saved. The load is applied as an area load p with a width of 1m and an amplitude of 80kN/m on the existing strip foundation. Since it is a strip foundation, the surface loads are typically provided per meter. The used soil model is hypoplastic with material transition from natural soil to cemented soil.[15] The transition from soil to concrete takes place by changing the temperature field in ABAQUS which is coupled

TABLE 3 Material parameters for sand and structural material according to Pucker.[15]

Material	p_0	e_c	ν_E	C_{c0}	φ_c	a	a_{Cc}	$\eta_{\max}$	a_φ	c'
Parameter	[kPa]	[-]	[-]	[-]	[°]	[-]	[-]	[-]	[-]	[kPa]
Sand	100	0,7	0,5	0,0056	32,0	0,22	1,16	3,63	3,85	0
Foundation	3300	0,7	0,3	0,0056	32,5	0,00	0,00	1,00	0,00	2200

10970207, 2024, 6, Downloaded from https://onlinelibrary.wiley.com/doi/10.1002/nme.7410 by Technische Universität Hamburg Universitätsbibliothek, Wiley Online Library on [04/03/2025]. See the Terms and Conditions (https://onlinelibrary.wiley.com/terms-and-conditions) on Wiley Online Library for rules of use; OA articles are governed by the applicable Creative Commons License

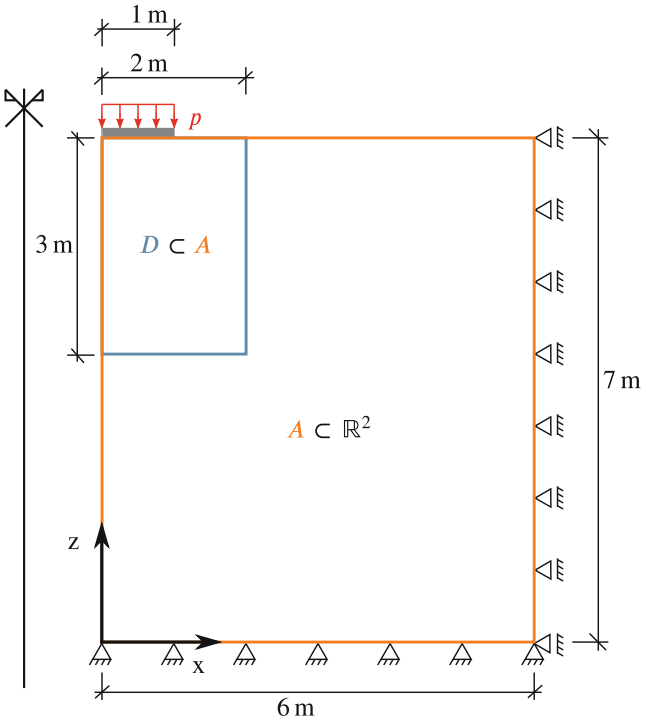

FIGURE 5 ABAQUS model of the strip foundation, with load p, the axis of symmetry, dimensions, boundary conditions, and the notation of design space and discretized area in ABAQUS.

with the used soil model. Thus, the temperature is used in the sense of a scalar field for interpolation and communication reasons between the soil model (subroutine) and the finite element (FE) model. With respect to this article, this has no meaning in the sense of thermodynamics. The temperature field is controlled by the virtual density, an output of the optimization algorithm.

3.2 | Setup of optimization algorithms

The coupling of the boundary value problem in ABAQUS with the two optimization algorithms in MATLAB is shown in the flowchart of Figure 6.

Similar to the discretization of the FE-model (cf. Figure 5), a discretization is also created in MATLAB that has the same dimensions as the area in ABAQUS. The fundamental difference here is, however, that the entire domain $M \subset \mathbb{R}^2$, which has the size of $A \subset \mathbb{R}^2$, is discretized equally fine over the whole solution space. The reason for this is the complexity that would be involved in creating an irregular mesh in MATLAB, which is not related to the orientation and structural storage required. This is because the discretization in MATLAB is not used for approximating of the physics. The actual design space D nevertheless exhibits the same mesh structures as the corresponding domain in ABAQUS. For the remaining domains, the values are interpolated to the respective elements or nodes when switching between MATLAB and ABAQUS. In this case a linear interpolation, the so-called "Shepard interpolation" is used with MATLAB.[27] An extrapolation formula of first-order can be derived from the Taylor series development up to the first term. At this point, it should be mentioned that the indices indicate the definition space of the respective quantity. The index i refers to the nodes and the index e is the summation over elements. Depending on the requirements and constraints of the implementation, the quantities are transformed accordingly between the different spaces. In MATLAB the initialization of the virtual density x takes place before the first FE calculation, depending on when the defined maximum permissible volume fraction starts. This volume fraction defines which proportion of the design space is available for the formation of the foundation structure. The described discretization is the same for the SIMP, SKO, and TOSS optimization. The flowchart in Figure 1 shows the coupling between ABAQUS and the three optimization algorithms in MATLAB. The shown procedure of the SIMP algorithm is used similarly in Pucker[15] and Seitz.[28] The virtual density which is a result of the optimization algorithm and

10970207, 2024, 6, Downloaded from https://onlinelibrary.wiley.com/doi/10.1002/nme.7410 by Technische Universität Hamburg Universitätsbibliothek, Wiley Online Library on [04/03/2025]. See the Terms and Conditions (https://onlinelibrary.wiley.com/terms-and-conditions) on Wiley Online Library for rules of use; OA articles are governed by the applicable Creative Commons License

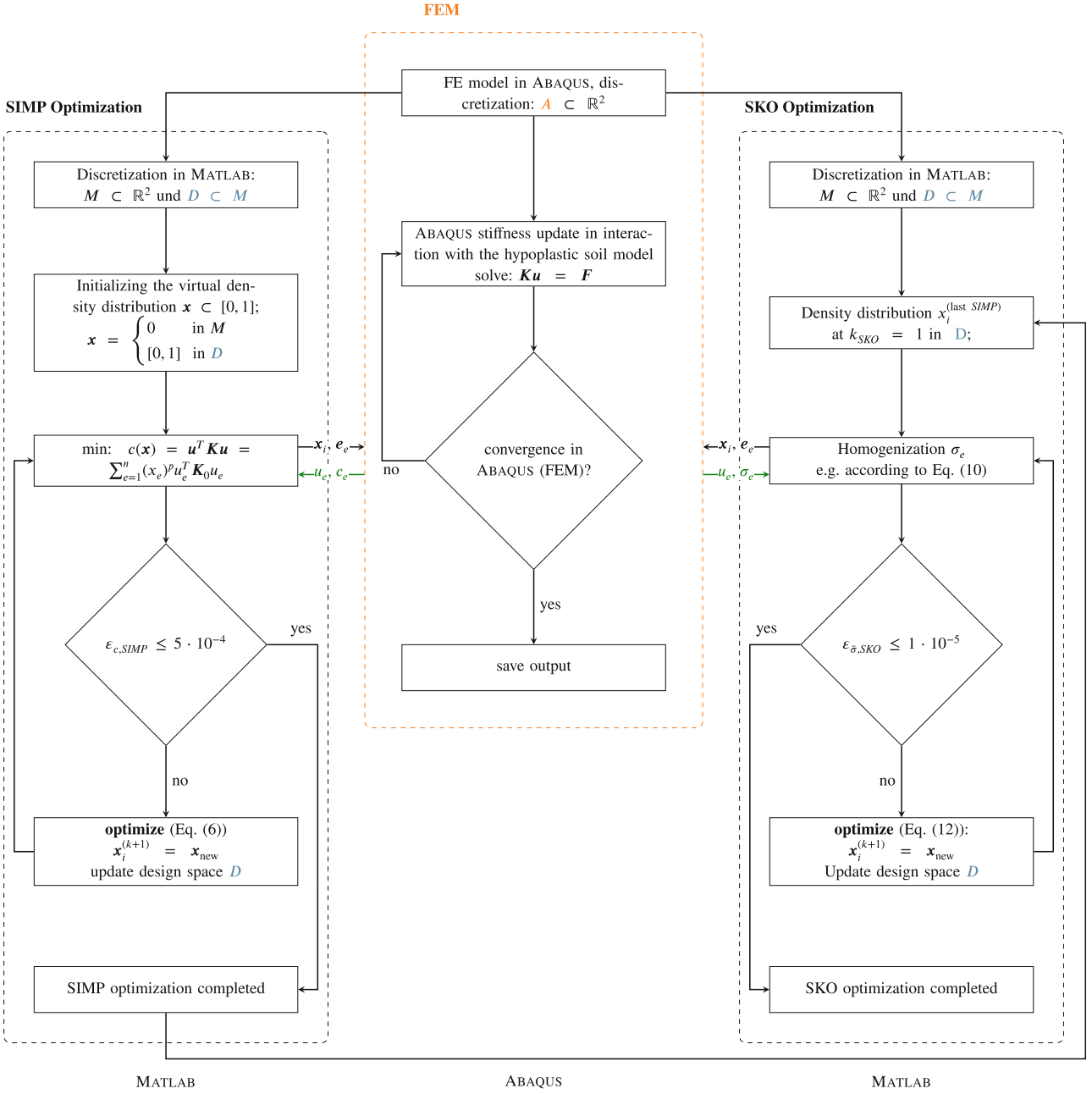

FIGURE 6 Flowchart of the hybrid algorithm using the SIMP method and subsequently the SKO method.

has values between $x_{min} \approx 0$ and 1 is forwarded to ABAQUS by writing the corresponding values as a file of the temperature field. The SIMP optimization is terminated as soon as the defined termination criterion is fulfilled. Usually, the number of iterations, which is defined by the user at the beginning of a calculation, is used as the termination criterion. Controlling the duration of an algorithm with the number of iterations carries the risk that a calculation is terminated too early or late. Terminating the calculation too early may not show the convergence yet, and terminating the calculation too late adds unnecessary calculations, increasing the calculation costs and time. For this reason, a convergence criterion is used as the termination criterion during the SIMP algorithm, which is defined in equation (13). The termination is controlled by the change in the calculated compliance $c(x)$. The convergence criterion is fulfilled if the change in compliance is less than 5×10^{-4} (cf. Equation (13)).

$$\varepsilon_{c,\mathrm{SIMP}} = 0.5 \frac{|c(x)^{(k_{\mathrm{SIMP}})} - c(x)^{(k_{\mathrm{SIMP}}-1)}|}{c(x)^{(k_{\mathrm{SIMP}}=1)}} + 0.5 \frac{|c(x)^{(k_{\mathrm{SIMP}}-1)} - c(x)^{(k_{\mathrm{SIMP}}-2)}|}{c(x)^{(k_{\mathrm{SIMP}}=1)}}. \tag{13}$$

10970207, 2024, 6, Downloaded from https://onlinelibrary.wiley.com/doi/10.1002/nme.7410 by Technische Universität Hamburg Universitätsbibliothek, Wiley Online Library on [04/03/2025]. See the Terms and Conditions (https://onlinelibrary.wiley.com/terms-and-conditions) on Wiley Online Library for rules of use; OA articles are governed by the applicable Creative Commons License

Coupling the SKO optimization algorithm to the boundary value problem in ABAQUS is technically similar to the coupling of SIMP and ABAQUS with the main difference being that the forwarded interpolation field is a result of an empirical optimization algorithm. Also in this case, the design space is updated according to the solution of the optimization algorithm. Since the homogenization of the stress state describes the objective function in SKO optimization, the convergence criterion is developed for evaluation. Through the application of the SKO optimization, an approximation of the existing stresses of the selected reference stress σ_{ref} is reached. If all the existing stresses in the design space are averaged, the average stress should settle as a value close to the reference value. For this reason, the stress $\overline{\sigma}_{zz}$ averaged over the elements e is used to evaluate the objective function. Normalized to the stress state, which is present after the last iteration of the SIMP optimization, the evaluation of the homogenized stress state results in the following equation

$$\overline{\sigma}_{zz} = \frac{\overline{\sigma}^{(k_{\text{SKO}})}}{\overline{\sigma}^{(k_{\text{SIMP,end}})}}. \tag{14}$$

As convergence criterion is fulfilled, the change in homogenization $\varepsilon_{\overline{\sigma},\text{SKO}}$ over the iteration steps k is used, compare (15). If $\varepsilon_{\overline{\sigma},\text{SKO}}$ is less than 1×10^{-5}, the optimization process is terminated.

$$\varepsilon_{\overline{\sigma},\text{SKO}} = \overline{\sigma}_{zz}^{(k_{\text{SKO}})} - \overline{\sigma}_{zz}^{(k_{\text{SKO}}-1)}. \tag{15}$$

4 | NUMERICAL IMPLEMENTATION

4.1 | Evaluation criteria

In order to evaluate and compare the optimized results, uniform evaluation criteria must be defined. Since the SIMP optimization algorithm aims to minimize the compliance of a structure, the settlement s of the strip foundation is chosen as a value for evaluation. The settlement of the rigid strip foundation is defined as

$$s(\boldsymbol{x}) = \frac{1}{n} \cdot \sum_{i=1}^{n} \begin{pmatrix} 0 \\ 1 \\ 0 \end{pmatrix}^{\text{T}} u_i(\boldsymbol{x}). \tag{16}$$

Here n is the number of nodes that are affected by the settlement of the strip foundation. Thus, $s(\boldsymbol{x})$ is the averaged settlement of the rigid strip foundation. As a second evaluation criterion, the volume of the structure is used, defined as

$$v(\boldsymbol{x}) = \sum_{n=1}^{e} x_n. \tag{17}$$

The volume of the structure is calculated based on the virtual density $\boldsymbol{x} = (x_1, \ldots, x_e)$ and defines which part of the design space is filled with structural material. The remaining area in the design space is filled with soil.

Finally, the evaluation of the objective function of the TOSS optimization is required. The first part of the *TOSS* optimization SIMP is evaluated in terms of the compliance $c(\boldsymbol{x})$ and of the volume of the structure $v(\boldsymbol{x})$. The second part, the SKO optimization, aims for a homogeneous stress state. As an evaluation criterion for SKO optimization, the mean stress in the design space ($\overline{\sigma}_{zz}$) is used, calculated with

$$\overline{\sigma}_{zz} = \frac{1}{e} \cdot \sum_{n=1}^{e} \begin{bmatrix} 0 & 0 & 0 \\ 0 & 1 & 0 \\ 0 & 0 & 0 \end{bmatrix} \sigma(x_n). \tag{18}$$

To be able to interpret the results independent of the quantities, the quantities are presented normalized to the first value of the SIMP optimization ($k = 1$) which guarantees comparability. The values will be used later on to evaluate the performed optimizations SIMP, TOSS, and SKO. With respect to the initial situation, the model is first computed without

10970207, 2024, 6, Downloaded from https://onlinelibrary.wiley.com/doi/10.1002/nme.7410 by Technische Universität Hamburg Universitätsbibliothek, Wiley Online Library on [04/03/2025]. See the Terms and Conditions (https://onlinelibrary.wiley.com/terms-and-conditions) on Wiley Online Library for rules of use; OA articles are governed by the applicable Creative Commons License

a foundation structure, which is the zeroth iteration step, $k = 0$ with $\boldsymbol{x} = \mathbf{0}$ (consequently $v(\boldsymbol{x}) = 0$). The mean settlement of the strip foundation is calculated here to be $s(\boldsymbol{x} = \mathbf{0}) = -0.0336$ m. The mean compliance of the system over the design space is $c(\boldsymbol{x} = \mathbf{0}) = 1.0543$ kJ.

4.2 | Parametric study

A parametric study is performed to set the values of the parameters s, the scaling factor and the reference stress, σ_{ref} in such a way that the interaction of these under the respective conditions fit the optimization problem as best as possible. The parameters are varied according to the values listed in Table 4. It should be noted, that the scaling factor is initially assumed for the determination of the reference stress as $s = 0.02$. After a suitable reference stress has been determined, the scaling factor is set. In order to determine possible reference stresses, the stress state in the $k = 45$ iteration of the SIMP optimization was used, shown in Figure 7. As the scale shows, the state contains vertical stresses up to −657kPa. It can be clearly seen that the greatest stresses occur in the area of the previously formed structure. In the surrounding area, where only soil material is present, the stresses are much lower. The dashed lines at the right and bottom edges indicate the transition to the entire model space, while the prolongation of the z-axis represents the symmetry axis. Stress distributions in these areas are irrelevant and are therefore not included. On the basis of the distribution, the selection of the reference stresses as shown in Table 4 is made.

Variation of the reference stress σ_{ref}

The reference stress σ_{ref} is varied according to the values of Table 4. The calculations are terminated after the convergence criterion was reached or after $k = 50$ iterations were carried out, since the first iterations are indicative for assessing the influence of the reference stress. Thereby, the calculations converge for $\sigma_{\text{ref}} = 120$ kPa and $\sigma_{\text{ref}} = 180$ kPa. The calculations with reference stresses of $\sigma_{\text{ref}} = 150$ kPa and $\sigma_{\text{ref}} = 200$ kPa are terminated after $k = 50$ iterations, since they do

TABLE 4 Parametric study: Variation of the reference stress σ_{ref} and the scaling factor s.

σ_{ref} [kPa]	120	150	180	200	
s	0.5	2	5	8	10

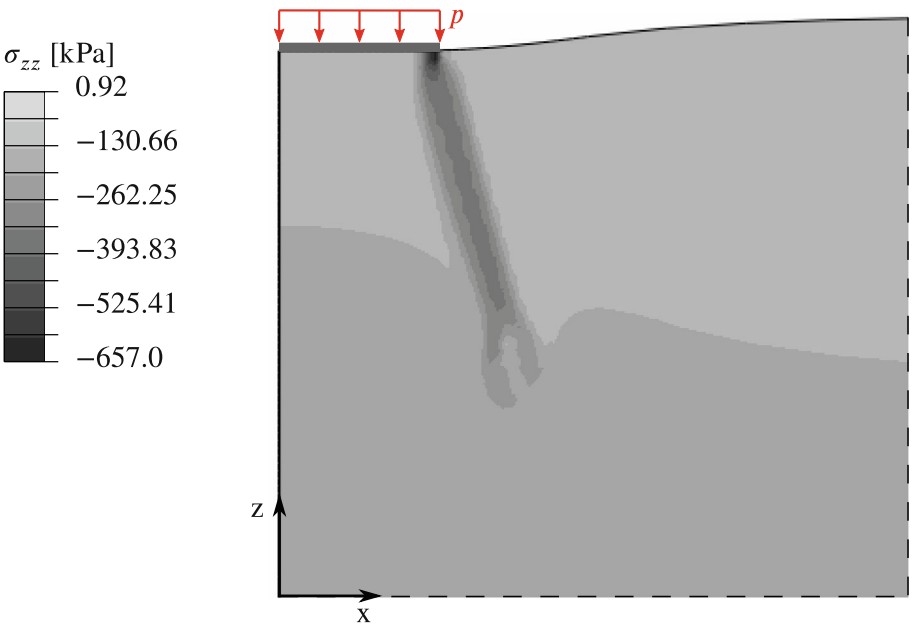

FIGURE 7 Stress distribution (σ_{zz}) in the design space, obtained after $k = 45$ iterations with the SIMP optimization.

10970207, 2024, 6, Downloaded from https://onlinelibrary.wiley.com/doi/10.1002/nme.7410 by Technische Universität Hamburg Universitätsbibliothek, Wiley Online Library on [04/03/2025]. See the Terms and Conditions (https://onlinelibrary.wiley.com/terms-and-conditions) on Wiley Online Library for rules of use; OA articles are governed by the applicable Creative Commons License

not reach convergence until this iteration. Nevertheless, it can be stated that the choice of a very small reference stress $\sigma_{\text{ref}} = 120$ kPa converges towards the trivial solution, as an extreme volume increases. In contrast, the calculations of the first iterations with high reference stresses ($\sigma_{\text{ref}} = 200$ kPa) show an extreme volume decrease. This indicates that the other trivial solution where there is no use of structural material in the design space, is being generated.

Within the parametric study of the reference stress variation, it became obvious that the compliance at smaller reference stresses drops sharply in the first iterations of the SKO optimization, then approaches a steady level. The volume develops similarly. The investigations of the different reference stresses have shown that its influence varies. For low reference stresses, the compliance c decreases and the volume v of the structure increases. For large reference stresses, the opposite trend is observed as shown in Figure 8.

Here, the relative changes in compliance, volume, and mean stress are plotted as a function of the reference stress σ_{ref}. The relative change is calculated to the results of the last iteration of the SIMP optimization ($k = 46$). Here, $\phi(\boldsymbol{x}) \in \{c(\boldsymbol{x}), v(\boldsymbol{x}), \overline{\sigma}_{zz}(\boldsymbol{x})\}$ acts as a generic quality function. The normalized relative change is then calculated as defined in the following.

$$\delta(\boldsymbol{x}) = \frac{\phi(\boldsymbol{x})^{k}}{\phi(\boldsymbol{x})^{\text{SIMP,last}}} - \frac{\phi(\boldsymbol{x})^{\text{SIMP,last}}}{\phi(\boldsymbol{x})^{\text{SIMP,last}}}. \tag{19}$$

The magnitude of the relative change is shown in Figure 8 on the ordinate. The abscissa gives information about the different reference stresses σ_{ref}. Depending on the hatching, the magnitudes of the mean stresses, compliance and volume are listed. Also, this figure shows the opposite evolution of the compliance c and the volume v. Moreover, the mean stresses at extreme reference stresses show the largest changes. It can also be seen very clearly that $\delta(\boldsymbol{x})$ of compliance $c(\boldsymbol{x})$ is smallest for the reference stress $\sigma_{\text{ref}} = 180$ kPa. The relative change in volume is also the smallest here, whereas the volume decreases significantly. With regard to the optimization objective of minimizing the compliance and simultaneously obtaining a homogeneous stress state, it is found, based on the results of the parameter study, that a reference stress of $\sigma_{\text{ref}} = 180$ kPa is most suitable for achieving the optimization objective of the hybrid approach under the described load case and previously defined parameters. This occurs due to a small change $\delta(\boldsymbol{x})$ in the compliance $c(\boldsymbol{x})$ (the optimization result of the SIMP optimization is thus still taken into account), therefore reducing the volume by the homogenization of the stresses. Moreover, it should be noted here that the change in compliance, in this case, is negative, resulting in smaller compliance than in the SIMP optimization.

Variation of the scaling factor

Since the previous investigations have shown that $\sigma_{\text{ref}} = 180$ kPa is a suitable reference stress, the investigations of the scaling factor s are performed using this reference stress. The scaling factor is calculated according to the varied parameters given in Table 4. The parameter study is evaluated according to the example of the reference stresses.

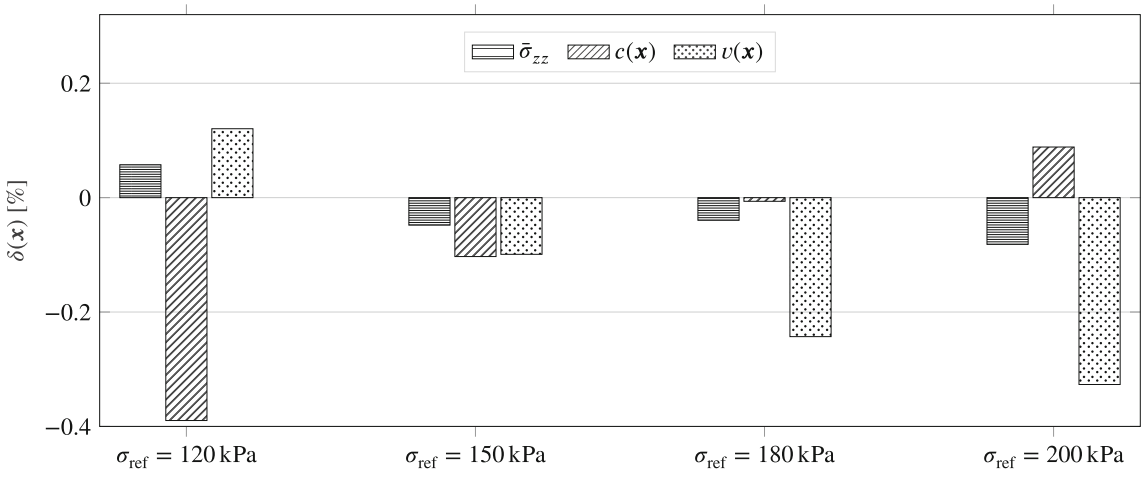

FIGURE 8 Relative change in the mean stress $\overline{\sigma}_{zz}$, compliance $c(\boldsymbol{x})$, and settling $s(\boldsymbol{x})$ for different reference stresses σ_{ref}.

10970207, 2024, 6, Downloaded from https://onlinelibrary.wiley.com/doi/10.1002/nme.7410 by Technische Universität Hamburg Universitätsbibliothek, Wiley Online Library on [04/03/2025]. See the Terms and Conditions (https://onlinelibrary.wiley.com/terms-and-conditions) on Wiley Online Library for rules of use; OA articles are governed by the applicable Creative Commons License

From the variation of the scaling factor, it can be seen that the scaling factor has a major influence on the first iterations. The smaller s is, the more $c(\boldsymbol{x})^{(k)}/c(\boldsymbol{x})^{(1)}$ decreases in the first iteration and the smaller the volume increase of structural material is. For large scaling factors (here $s = 10/100$), an opposite trend is observed.

Nevertheless, the influence of the large scaling factor can be seen. The volume increases extremely, and the compliance decreases in the first iterations. This correlation is due to the influence that the scaling factor has on the SKO optimization. It influences how much the difference of existing stress to the reference stress is weighted in the update of the virtual density. Since in this case, the difference in stresses remains the same (since $\sigma_{\text{ref}} = 180$ kPa is assumed to be constant) a larger scaling factor should increase the influence, while smaller scaling factors should decrease the influence. This relationship implies that using smaller s will result in small changes. Due to the empirical approach, which the SKO optimization entails, the computations again come out of the minimum, which they approach in the first iteration. This would not be possible with a deterministic approach, such as that used in SIMP optimization. Only the highest scaling factor shows different behavior. In the specified range (between $s = 0.5/100$ and $s = 5/100$) the choice of the scaling factor does not have too much influence on the calculations. The sizes of the scaling factor, which are in the size range of the virtual density are the only saying factors that steeply influence the calculations.

The variation of the reference stress shows that the reference stress has a major influence on the calculations, which underlines the importance of choosing an appropriate reference stress. The choice of the scaling factor is less sensitive than the reference stress.

Based on the results of the parameter study, $\sigma_{\text{ref}} = 180$ kPa and $s = 2/100$ are established for future calculations of the boundary value problem "strip foundation" with the TOSS optimization and the given load case.

4.3 | Results and discussion

It should be noted here that the following results refer to SIMP and SKO in the context of a coupled optimization and not to a single optimization. All the results in the course of the tabular comparison (cf. Table 5), as well as the results of the individual optimizations of SIMP and SKO, as the results of the coupled TOSS optimization, are used. For all optimizations the results are compared with values of the compliance $c(\boldsymbol{x})$ [kJ], the change in settlement Δs^0 [cm], and the used structural volume [%]. Here, Δs^0, is defined as the change in settlement compared to the initial state (soil only), which is also listed. The change in settlement is used because it is a significant parameter to evaluate the performance of a foundation. The structural volume is defined as the percentage ratio of the virtual density in the design space to the initial volume V^0 (total design space with soil). For the pure SIMP and SKO optimizations, no convergence criteria are used. Due to this, both optimizations are terminated after 60 iterations.

The results of the hybrid optimization process regarding the normalized compliance, settlement and volume are shown in Figure 9. The blue lines show the results of the first part of the TOSS optimization, the SIMP, whereas the red curves show those of the following SKO part.

It can be seen that the compliance (cf. Figure 9A) and the settlement (cf. Figure 9B), develop qualitatively similar in both parts of the optimization. Both blue curves show a noticeable jump at about the 10th iteration and decrease steadily from there on. Smaller jumps at the 20th and 40th iteration steps are also present. The red part of the curves also quite similar in quality. The range in values differ in both parts of the optimization. The initially declining compliance in Figure 9A is due to the material redistribution of the SIMP optimization. Starting from an evenly distributed virtual density, a topology develops which is forced by the penalty term p to assume virtual densities close to $\boldsymbol{x} = 1$ or $\boldsymbol{x} = \boldsymbol{x}_{\text{min}} \approx 0$,

TABLE 5 Summary of the results of the boundary value problem "strip foundation" based on the parameters: Iteration step k, average compliance $c(\boldsymbol{x})$, change of settlement Δs^0, and structural volume $v(\boldsymbol{x})$.

Optimization	k	$c(\boldsymbol{x})$ [kJ]	Δs^0 [cm]	$v(\boldsymbol{x})$ [%]
Initial state	0	1.0543	-	-
SIMP	60	0.3282	2.09	10.06
SKO	60	0.2080	2.32	10.29
TOSS (part 1: SIMP)	45	0.3233	2.10	10.05
(part 2: SKO)	77	0.3223	2.14	7.62

10970207, 2024, 6, Downloaded from https://onlinelibrary.wiley.com/doi/10.1002/nme.7410 by Technische Universität Hamburg Universitätsbibliothek, Wiley Online Library on [04/03/2025]. See the Terms and Conditions (https://onlinelibrary.wiley.com/terms-and-conditions) on Wiley Online Library for rules of use; OA articles are governed by the applicable Creative Commons License

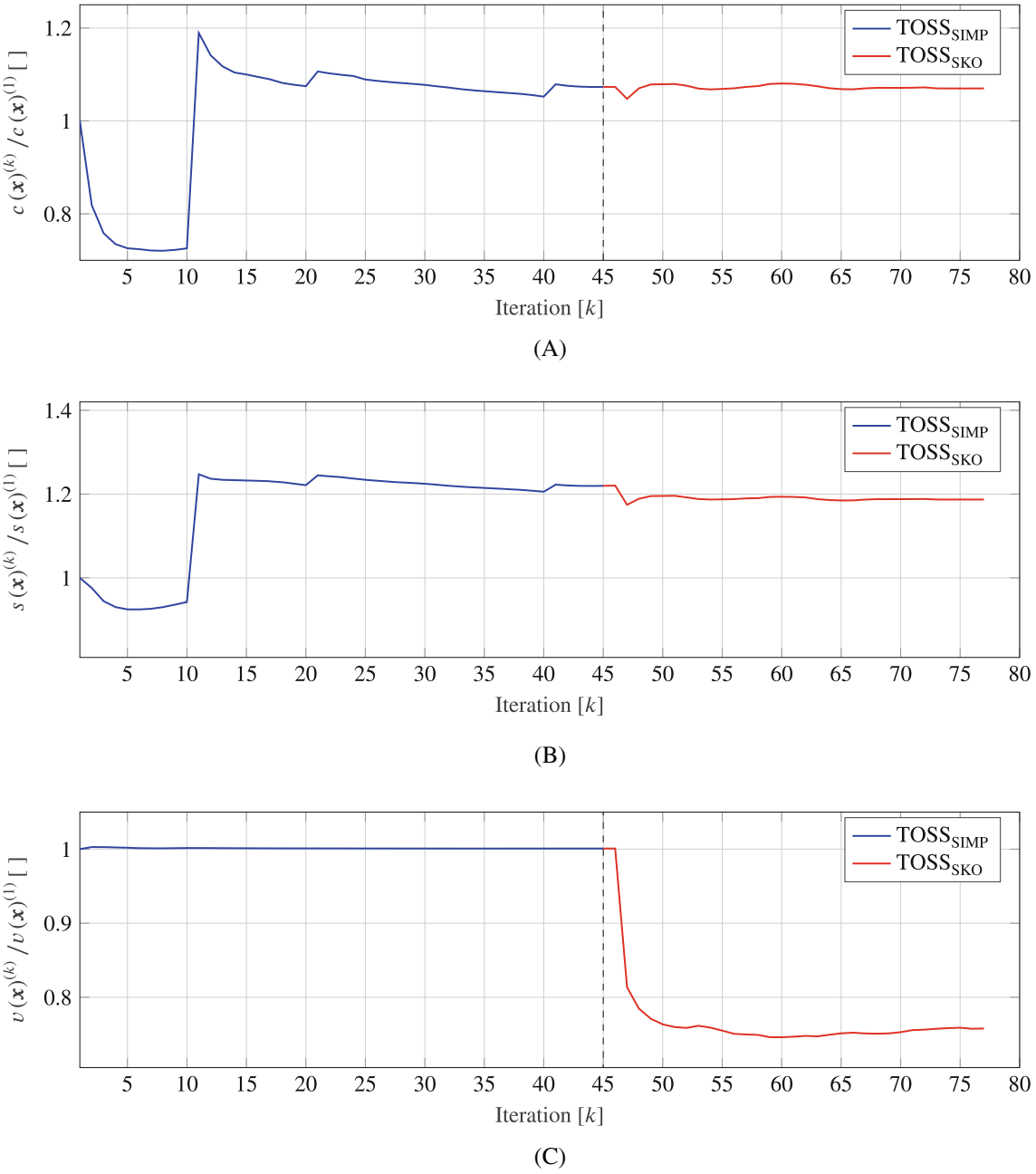

FIGURE 9 Results of the TOSS optimization with $k_{\text{SIMP}} = 45$ and $k_{\text{SKO}} = 32$ iterations ($k = 77$). (A) Change of $c(\boldsymbol{x})^{(k)}/c(\boldsymbol{x})^{(1)}$ over $k = 77$ iterations. (B) Change of $s(\boldsymbol{x})^{(k)}/s(\boldsymbol{x})^{(1)}$ over $k = 77$ iterations. (C) Change of $v(\boldsymbol{x})^{(k)}/v(\boldsymbol{x})^{(1)}$ over $k = 77$ iterations.

to get a discretized field. Starting with a low penalty term, this is raised with increasing iterations (continuation method, cf. Table 1). This prevents too many elements from being forced to take on a certain value too early. At this point in time, many elements in the design space are still filled with intermediate materials accordingly. This implies a larger area of material that has higher stiffnesses than that of the soil. The compliance is low here and as the iteration increases, the virtual density is redistributed in a way that more elements have discrete values. This is due to the application of a penalty function that is not constant. The penalty function is increased at iteration $k = 10$, $k = 20$, $k = 30$, and $k = 40$ iterations. Thus, a small jump in the results of compliance and settlement can be seen exactly at these points.

The initial jump in the SIMP results at $k = 10$ is smaller in the development of the settlement than with respect to the compliance. The reason for this is that the compliance results as an averaged element size from the FE calculation, while the settlement results as a size averaged over the FE nodes according to Equation (16). The initial jump in the SIMP results is smaller for the development of the settlement compared to the jump in compliance. The jumps have relatively

10970207, 2024, 6, Downloaded from https://onlinelibrary.wiley.com/doi/10.1002/nme.7410 by Technische Universität Hamburg Universitätsbibliothek, Wiley Online Library on [04/03/2025]. See the Terms and Conditions (https://onlinelibrary.wiley.com/terms-and-conditions) on Wiley Online Library for rules of use; OA articles are governed by the applicable Creative Commons License

small magnitudes. Additionally, the normalization of the values is carried out according to the first value ($k = 1$) of the specific parameter. Quantitative differences in the curves are to be expected thereby.

The volume, on the other hand, remains relatively constant during the SIMP optimization (blue), fluctuations in the volume here are in ranges with a scale of 10^{-3} (cf. Figure 9C). This behavior is due to the volume constraint used.

The subsequent SKO optimization (red curves) shows that first the respective values of compliance, settlement and volume of the last iteration of the SIMP optimization are used for the first iteration of the SKO optimization. Thus, a continuous transition can be seen. From there, the compliance as well as the settlement continue to develop at a relatively constant level, except for a local drop at the beginning of the SKO optimization. In contrast, the volume decreases continuously during the SKO optimization and settles at a constant level at around $k = 55$. Furthermore, the SKO optimization was independently investigated in order to examine the influence of the SKO optimization without the preceding SIMP optimization and on the considered boundary value problem. For this purpose, the corresponding constraints or transition conditions were adapted, since the SKO calculation was no longer a subsequent step.

The comparison between SKO within the TOSS algorithm and SKO as a single optimization algorithm shows an important difference. When using SKO in the coupled framework of TOSS a constraint regarding the maximum compliance is added. The reason for this is to prevent that the modified compliance as a result of SIMP optimization is degraded. As a result of this constraint, the structure does not grow to the edge of the design space within the TOSS optimization. Thus, there are no boundary influences. However, using pure SKO optimization leads to structures that grow to the edge of the design space, since there is no corresponding constraint. Consequently, boundary influences cannot be excluded when using SKO in an uncoupled framework.

According to Equation (18), the homogenization of the stresses is evaluated in the framework of the SKO optimization. Figure 10 shows the development of the mean stress $\overline{\sigma}_{zz}$ in the SKO calculation part of the TOSS optimization. From Figure 10 it can be seen that the mean stress decreases steadily until it settles to a constant level from about the 28th iteration. The stress homogenization aimed at by the SKO is thus also fulfilled in the coupled optimization.

When considering all three figures of the TOSS optimization as a whole, it becomes clear that the courses of the functions remain constant for the first iteration of the SKO calculation. This shows that the state transfer between the computational algorithms is correct. In the next iteration step, the influence of the SKO optimization is clearly visible for all functions. The normalized change in compliance (cf. Figure 9A) and settlement (cf. Figure 9B) behave similarly across all iterations. Both graphs drop significantly with the first iteration, but return to almost the initial level of the last SIMP iteration in the course of subsequent iterations. However, the function of the normalized volume ($v(x)^{(k)}/v(x)^{(1)}$, compare Figure 9C), remains at a low level after the sharp drop during the first iterations of the SKO optimization and converges here. In summary, the results of the optimization are shown in Table 5. The results also show that using the TOSS algorithm leads to 7.62% volume of structural material, whereas using only one optimization algorithm leads for the same case to more than 10% volume of structure material, leading to 24% volume savings when applying the TOSS algorithm.

The main focus is the foundation structure, which is obtained after the entire TOSS optimization, compare Figure 11. The surface of the SIMP structure (cf. Figure 11A) remains similar and throughout the downstream SKO part (cf. Figure 11B), a pile-like foundation shape remains. By direct comparison, it is clear that the structure is somewhat narrower overall. This structure geometry is especially observed in the area of load introduction, at the top of the design space

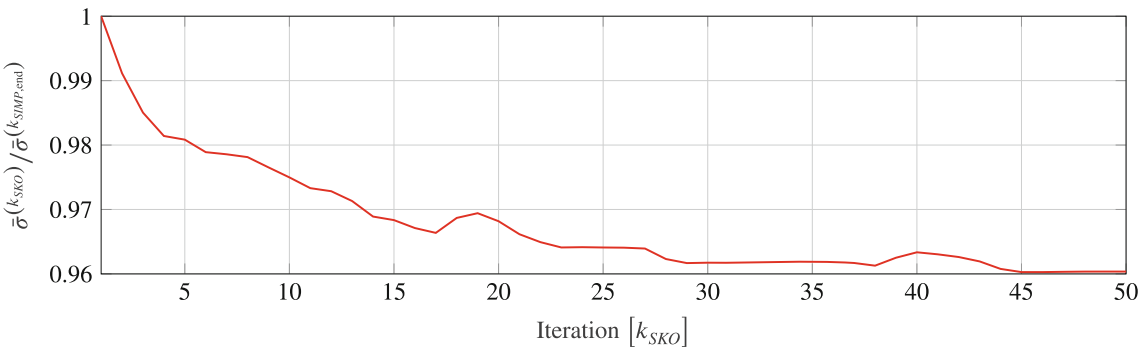

FIGURE 10 Development of the mean stresses $\overline{\sigma}_{zz}$ as a measure of the homogeneous stress state in the design space during the TOSS optimization.

10970207, 2024, 6, Downloaded from https://onlinelibrary.wiley.com/doi/10.1002/nme.7410 by Technische Universität Hamburg Universitätsbibliothek, Wiley Online Library on [04/03/2025]. See the Terms and Conditions (https://onlinelibrary.wiley.com/terms-and-conditions) on Wiley Online Library for rules of use; OA articles are governed by the applicable Creative Commons License

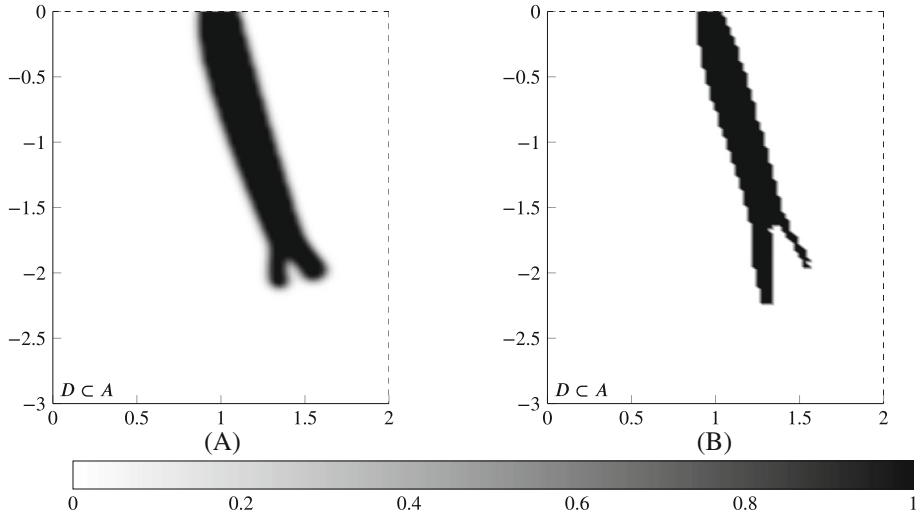

FIGURE 11 Optimized topology of a foundation structure (based on the distribution of virtual density ($\boldsymbol{x}$)) using the TOSS optimization, after $k = 45$ iterations of the SIMP-optimization (A) and further $k = 32$ iterations of the SKO optimization (B). (A) $k_{\text{SIMP}} = 45$. (B) $k_{\text{SKO}} = 32$.

and towards the bottom of the foundation structure. The bifurcation formed during the SIMP optimization is further widened by the subsequent SKO optimization. A deeper branching is formed, whereby the right branching is significantly slimmer than the left one. The opposite is true for the foundation structure in Figure 11A. In addition, the ends are more pointed in comparison to the results of the SIMP optimization. Another clear difference is observed in the edge region of the structure. In Figure 11B, the edge region is not as smoothed as after the SIMP optimization. Here, the surface of the structure shows angular gradients. The reason for the difference in the smoothness of the edges is that the SIMP calculation is based on a filter, while the SKO calculation is not. Due to the filter, more intermediate materials also occur in the SIMP calculation than in the SKO calculation. The occurrence of the intermediate materials is due to the use of the continuous design variable, which is forced to discretize by the penalty function. The filter is only applied after the forced discretization and averages individual node values here. This creates intermediate materials that are not subsequently forced to discretize again, thus blurring the boundary region. The filter function depends on the discretization. The main differences between the structures formed from the individual optimization algorithms and the structure formed from the hybrid calculation are the slimmer dimensions and the bottom end of the structures. In conclusion, it should be noted that the optimization results based on the SIMP algorithm have been extensively investigated in Pucker[15] and their plausibility has been verified. The focus of this work lies in examining the differences between the SIMP and coupled TOSS algorithms. As the corresponding settlements for structures resulting from the coupled algorithm were numerically computed and validated, it can be inferred that the resulting structure underwent plausibility checks.

5 | CONCLUSION

Three different optimization algorithms (SIMP, SKO, and TOSS) in the framework of geotechnics are applied to the boundary value problem of a strip foundation and investigated. This work provides further evidence of the applicability of optimization algorithms in geotechnical engineering. The TOSS algorithm is a coupling of the SIMP and SKO algorithms and combines both objects of optimization, namely the reduction of the compliance of a structure and the homogenization of stresses, within one algorithm. In order not to degrade the modified results of the first SIMP calculation, constraints are introduced that limit the allowed compliance within the second SKO calculation. These special modifications not only allow structures to be maintained that are also used in optimization with the SIMP approach but also reduce the computing time. In addition, the reduction of many interpolations makes the practical applicability appealing. It was shown for the strip foundation boundary value problem considered in this case that useful and improved results can be obtained with coupled TOSS optimization compared to single optimization. The results show that higher material savings can be achieved by coupling the deterministic SIMP and empirical SKO calculations. Up to 24% more material savings can be

10970207, 2024, 6, Downloaded from https://onlinelibrary.wiley.com/doi/10.1002/nme.7410 by Technische Universität Hamburg Universitätsbibliothek, Wiley Online Library on [04/03/2025]. See the Terms and Conditions (https://onlinelibrary.wiley.com/terms-and-conditions) on Wiley Online Library for rules of use; OA articles are governed by the applicable Creative Commons License

achieved compared to a pure SIMP optimization. This is accompanied by savings in CO_2 emissions in relation to material consumption. Especially for large construction projects with large material usage, the 24% savings can translate to noticeable absolute material savings. However, it should be generally noted that the CO_2 savings due to pure material savings can be countered by increased manufacturing effort of the non-standard foundation construction. However, the direct comparison between the construction resulting from a SIMP optimization and a TOSS optimization shows no significant differences in execution, which is why the increased manufacturing effort can be understood as a general aspect related to optimized constructions. Although it could be shown that the coupling of SIMP and SKO optimization is technically possible, the sensitivity of the scaling factor and reference stress with respect to the SKO optimization are high. For this reason, these two quantities must be determined in advance as part of a parameter study, as was done in this study. The execution of the parameter studies is essential for the quality assurance of the results, otherwise, distorted results are possible. Since the optimization processes are coupled to an FE calculation, the quality of the results depends on the quality of the FE models.

DATA AVAILABILITY STATEMENT

Data sharing not applicable to this article as no datasets were generated or analyzed during the current study.

ACKNOWLEDGMENT

Open Access funding enabled and organized by Projekt DEAL.

ORCID

Elnaz Hadjiloo https://orcid.org/0000-0002-7088-4513

REFERENCES

1. Fletcher R. *Practical Methods of Optimization*. Wiley; 1987.
2. Harzheim L. *Strukturoptimierung: Grundlagen und Anwendungen*. Edition Harri Deutsch. 2nd ed. Verlag Europa-Lehrmittel - Nourney, Vollmer GmbH & Co. KG; 2014.
3. Schumacher A. *Optimierung Mechanischer Strukturen: Grundlagen Und Industrielle Anwendungen*. Springer eBook Collection Computer Science and Engineering. 2nd ed. Springer Vieweg; 2013.
4. Bendsøe MP, Kikuchi N. Generating optimal topologies in structural design using a homogenization method. *Appl Mech Eng*. 1988;71:197-224.
5. Sigmund O, Maute K. Topology optimization approaches. *Struct Multidiscipl Optim*. 2013;48(6):1031-1055. doi:10.1007/s00158-013-0978-6
6. Seitz KF. *Zur Topologieoptimierung von geotechnischen Strukturen und zur Tragfähigkeitssteigerung des Baugrunds durch Scherfugenverfestigung*. PhD Thesis. Technische Universität Hamburg, Institut für Geotechnik und Baubetrieb; 2020.
7. Deaton JD, Grandhi RV. A survey of structural and multidisciplinary continuum topology optimization: post 2000. *Struct Multidiscipl Optim*. 2013;49(1):1-38. doi:10.1007/s00158-013-0956-z
8. Eschenauer HA, Kobelev VV, Schumacher A. Bubble method for topology and shape optimization of structures. *Struct Optim*. 1994;8(1):42-51. doi:10.1007/bf01742933
9. Xie YM, Steven GP. A simple evolutionary procedure for structural optimization. *Comput Struct*. 1993;49(5):885-896.
10. Bendsøe MP. *Optimization of Structural Topology, Shape, and Material*. Springer; 1995.
11. Sigmund O. A 99 line topology optimization code written in Matlab. *Struct Multidiscipl Optim*. 2001;21(2):120-127. doi:10.1007/s001580050176
12. Siva Rama Krishna L, Mahesh N, Sateesh N. Topology optimization using solid isotropic material with penalization technique for additive manufacturing. *Mater Today Proc*. 2017;4(2):1414-1422. doi:10.1016/j.matpr.2017.01.163
13. Zhu J, Gao T, Zhang W. *Topology Optimization in Engineering Structure Design*. Elsevier Science; 2016.
14. Calì M, Oliveri S. Application of an effective SIMP method with filtering for topology optimization of motorcycle tubular frame. *Int Rev Mech Eng*. 2017;11:836. doi:10.15866/ireme.v11i11.13770
15. Pucker T. *Stoffmodell zur Modellierung von stetigen Materialübergängen im Rahmen der Optimierung geotechnischer Strukturen*. PhD Thesis. Techn. Univ. Hamburg-Harburg, Inst. für Geotechnik und Baubetrieb; 2013.
16. Wu Q, Zhou Q, Zhang R, Xiong X. Periodic topology optimization of crane boom based on improved soft kill option method. *J Shanghai Jiaotong Univ Sci*. 2017;22:459-465. doi:10.1007/s12204-017-1859-8
17. Harzheim L, Graf G. Optimization of engineering components with the SKO method. *SAE Trans*. 1995;104:1974-1982.
18. Baumgartner A, Harzheim L, Mattheck C. SKO (soft kill option): the biological way to find an optimum structure topology. *Int J Fatigue*. 1992;14(6):387-393. doi:10.1016/0142-1123(92)90226-3
19. Frisch M. *Entwicklung eines Hybridalgorithmus zur steifigkeits- und spannungsoptimierten Auslegung von Konstruktionselementen*. PhD Thesis. Universität Bayreuth, Lehrstuhl für Konstruktionslehre Und CAD; 2015.
20. Bendsøe MP. Optimal shape design as a material distribution problem. *Struct Optim*. 1989;1:193-202. doi:10.1007/BF01650949

10970207, 2024, 6, Downloaded from https://onlinelibrary.wiley.com/doi/10.1002/nme.7410 by Technische Universität Hamburg Universitätsbibliothek, Wiley Online Library on [04/03/2025]. See the Terms and Conditions (https://onlinelibrary.wiley.com/terms-and-conditions) on Wiley Online Library for rules of use; OA articles are governed by the applicable Creative Commons License

21. Grabe J, Seitz KF. Optimization of geotechnical structures for states of serviceability and ultimate loads. *6th International Conference on Structural Engineering, Mechanics and Computation, SEMC 2016*. CRC Press; 2016:2048-2053.
22. Sigmund O. Design of multiphysics actuators using topology optimization—part I: one-material structures. *Comput Methods Appl Mech Eng*. 2001;190(49-50):6577-6604. doi:10.1016/s0045-7825(01)00251-1
23. Rozvany GIN. A critical review of established methods of structural topology optimization. *Struct Multidiscipl Optim*. 2008;37(3):217-237. doi:10.1007/s00158-007-0217-0
24. Rosnitschek T, Hentschel R, Siegel T, et al. Optimized one-click development for topology-optimized structures. *Appl Sci*. 2021;11(5):2400. doi:10.3390/app11052400
25. Niemunis A. *Extended Hypoplastic Models for Soils*. PhD Thesis. Ruhr-Universität Bochum; 2003.
26. Dassault Systèmes. ABAQUS 6.11. Online Documentation; 2011. http://130.149.89.49:2080/v6.11/index.html
27. Shepard D. *A Two-Dimensional Interpolation Function for Irregularly-Spaced Data*. ACM Press; 1968.
28. Seitz KF, Pucker T, Grabe J. Topologieoptimierung in der Geotechnik: Anwendung auf Gründungsstrukturen und Validierung. *Geotechnik*. 2016;39(1):18-28. doi:10.1002/gete.201400031

How to cite this article: Hadjiloo E, Knutz S, Grabe J. Towards the saving potentials using a hybrid topology optimization: Application of a coupled deterministic and empirical approach solving a geotechnical optimization problem. *Int J Numer Methods Eng*. 2024;125(6):e7410. doi: 10.1002/nme.7410

10970207, 2024, 6, Downloaded from https://onlinelibrary.wiley.com/doi/10.1002/nme.7410 by Technische Universität Hamburg Universitätsbibliothek, Wiley Online Library on [04/03/2025]. See the Terms and Conditions (https://onlinelibrary.wiley.com/terms-and-conditions) on Wiley Online Library for rules of use; OA articles are governed by the applicable Creative Commons License